

Supplementary Information

Elucidating the formation of Al-NBO bonds, Al-O-Al linkages and clusters in alkaline-earth aluminosilicate glasses based on molecular dynamics simulations

Sudheer Ganiseti,^a Anuraag Gaddam,^b Rajesh Kumar,^c Sathravada Balaji,^d Glenn C. Mather,^e Maria J. Pascual,^e Margit Fabian,^f Renée Siegel,^g Jürgen Senker,^g Vladislav. V. Kharton,^h Julien Guénolé,ⁱ N. M. Anoop Krishnan^{d*}, José M. F. Ferreira,^{c*} Amarnath R. Allu,^{d*}

^a Department of Materials Science and Engineering, Institute I, Friedrich-Alexander-Universität Erlangen-Nürnberg, Martensstr. 5, 91058 Erlangen, Germany

^b Department of Materials and Ceramic Engineering, CICECO, University of Aveiro, 3810–193 Aveiro, Portugal

^c Department of Civil Engineering, Indian Institute of Technology Delhi, Hauz Khas, New Delhi, India 110016

^d Glass Division, CSIR-Central Glass and Ceramic Research Institute, 700032, Kolkata, India

^e Instituto de Cerámica y Vidrio (CSIC), C/Kelsen 5, Campus de Cantoblanco, 28049 Madrid, Spain

^f Centre for Energy Research, 1121 Budapest Konkoly-Thegest. 29-33, Hungary

^g Inorganic Chemistry III, University of Bayreuth, 95440 Bayreuth, Germany

^h Institute of Solid State Physics RAS, 142432 Chernogolovka, Moscow District, Russia

ⁱ Institute of Physical Metallurgy and Materials Physics, RWTH Aachen University, 52056 Aachen, Germany

*Corresponding author

Email: aareddy@cgcri.res.in (A. R. Allu)

Phone: +91–33–23223421; Fax: +91–33–24730957

Email: krishnan@iitd.ac.in (N. M. A. Krishnan)

Phone: +91–11–26591223;

Email: jmf@ua.pt (J.M.F. Ferreira)

Phone: +351-234-370242. Fax: +351-234-370204

S1: Reliability of Pedone potential

In order to check the reliability of Pedone potentials, a few samples of different compositions are prepared in two different cases and their structural properties compared with the experimentally available data from the literature.

Case 1: Three glass samples, chemical composition 29.4 Na₂O–29.4 Al₂O₃– 41.2 SiO₂, in mol %, were prepared each with 3588 atoms using Pedone potentials with a cooling rate of 5 K/ps following the preparation method mentioned in the manuscript. These three samples are prepared starting with different initial positions. The values of the O site population in Al–O–Al as estimated using the 3Q MAS NMR and computed from the MD simulations is presented in table S1.¹ The standard deviation is calculated using a total of three samples. From the experiments, 15% of O is found in the Al–O–Al bonds whereas the same obtained from simulations is 19.1%. The difference of 4% between simulations and experiments is not considered to be significant enough to reach any conclusions; this difference can be attributed to several factors such as the quantification procedure followed in the experiments, high cooling rates used in the simulations to prepare the glasses or the lack of polarization effects for oxygen atoms in the potential. Besides the quantitative difference, the RI potential (Pedone) qualitatively shows a significant number of Al–O–Al bonds.

Table S1: Comparison of O site population in Al–O–Al bonds.

Method Used	Al–O–Al
¹⁷ O 3Q MAS NMR	15 %
MD Simulations (Pedone)	19.1 %

Case 2: As part of case 2, two different glass compositions are prepared (compositions are given in the table below) with 3500 atoms using the Pedone potential with a cooling rate of 5

K/ps by following the preparation method mentioned in the manuscript. Three samples are prepared for each composition starting with three different initial samples. The percentage of Al with 4 and 5 coordinated O has been calculated and compared with the values extracted using ^{27}Al MAS NMR as reported by Kelsey et al², see table S2. The 5 coordinated Al obtained by MD simulations are very close to the experimental values for the S1 sample, whereas the simulations underestimate this value to a smaller amount in the S2 sample; however, qualitatively, the simulations show a similar trend of increasing the 5 coordinated Al atoms on replacing Ca with Mg. Also, in this case, the Pedone potential shows a very good qualitative agreement.

Table S2: Percentage of Al with 4 and 5 coordinated O.

Composition	Method Used	Al[4]	Al[5]
S1: 20 CaO – 20 Al ₂ O ₃ – 60 SiO ₂	^{27}Al MAS NMR	92.3	7.7
	MD (Pedone)	90.8±0.8	8.8±0.5
S2: 20 MgO – 20 Al ₂ O ₃ – 60 SiO ₂	^{27}Al MAS NMR	81.2	19.8
	MD (Pedone)	87±1.3	12.9±1.1

S2: Influence of interatomic potential

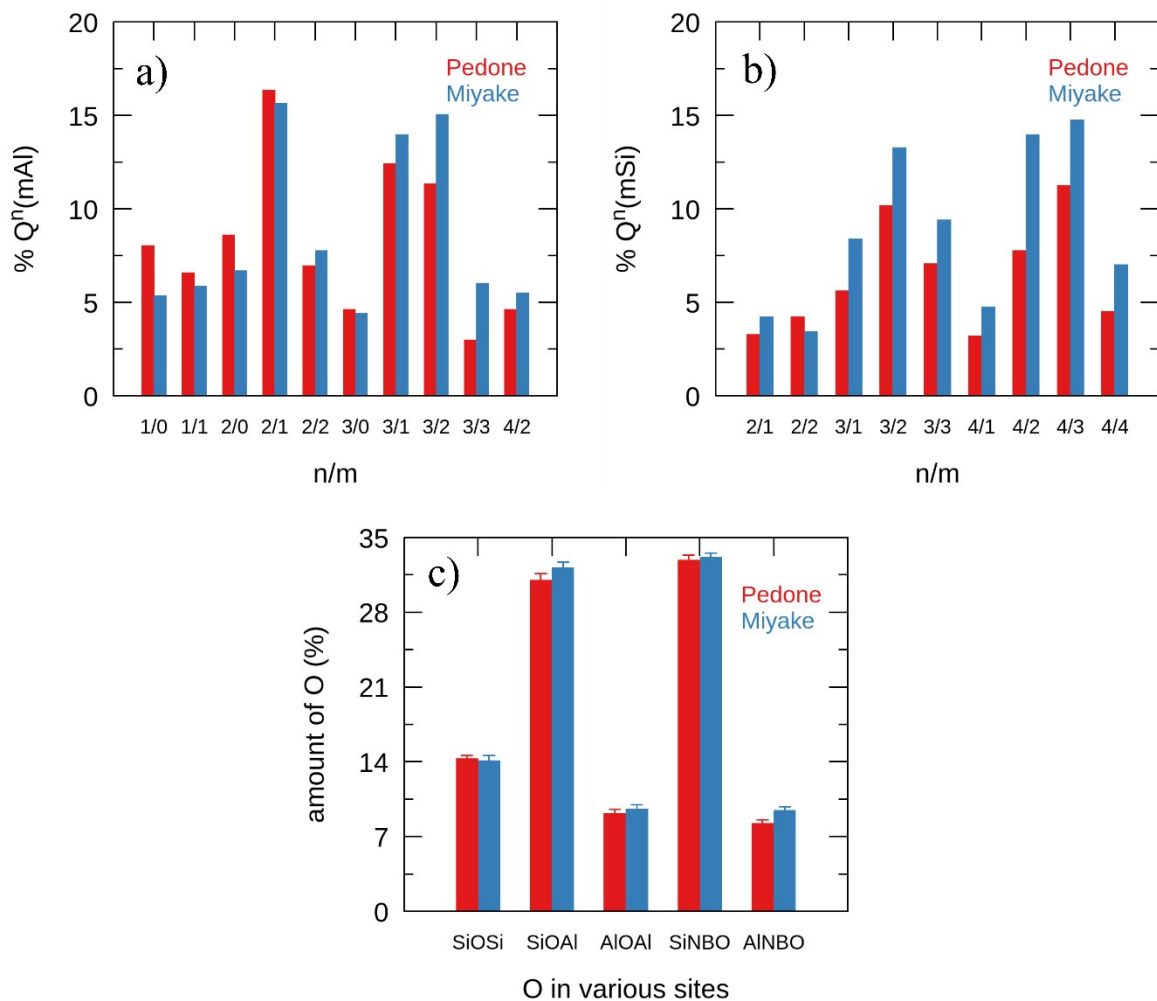


Figure S1: A comparison of (a) Q_{Si} , (b) Q_{Al} units distribution and (c) O in various sites is made between glasses prepared with Pedone and Miyake potentials.

The distribution of framework cations based on their neighbouring cations has been studied with two different potential models, namely Pedone and Miyake. Five samples are prepared with each potential to check the reproducibility and to minimize the statistical error. Fig. S1 shows the comparison of average distribution of Si and Al cations, based on their neighbouring cations, in the form of $Q^n(\text{mAl})$ (a) and $Q^n(\text{mSi})$ (b), respectively. The differences in the distribution of Si and Al between the Pedone and Miyake glasses within the RI model are very consistent with each other and within the deviation, except for the acceptable difference between $Q^3(2\text{Al})$ and $Q^4(2\text{Si})$ units. The amount of oxygen existing in various sites, Si–O–Si, Si–O–Al, Al–O–Al, Si–NBO and Al–NBO, is compared in the

glasses prepared with Pedone and Miyake potentials in Fig. S1(c). It shows that both models are in good agreement. Although the potential models are built fundamentally on different physical aspects, quantitatively, the distribution of framework cations shows very small differences, whereas qualitatively both glasses show a similar behaviour. We consider, therefore, that the potentials provide reliable results in the present study to support the EMRN model.

S3: Influence of cooling rate

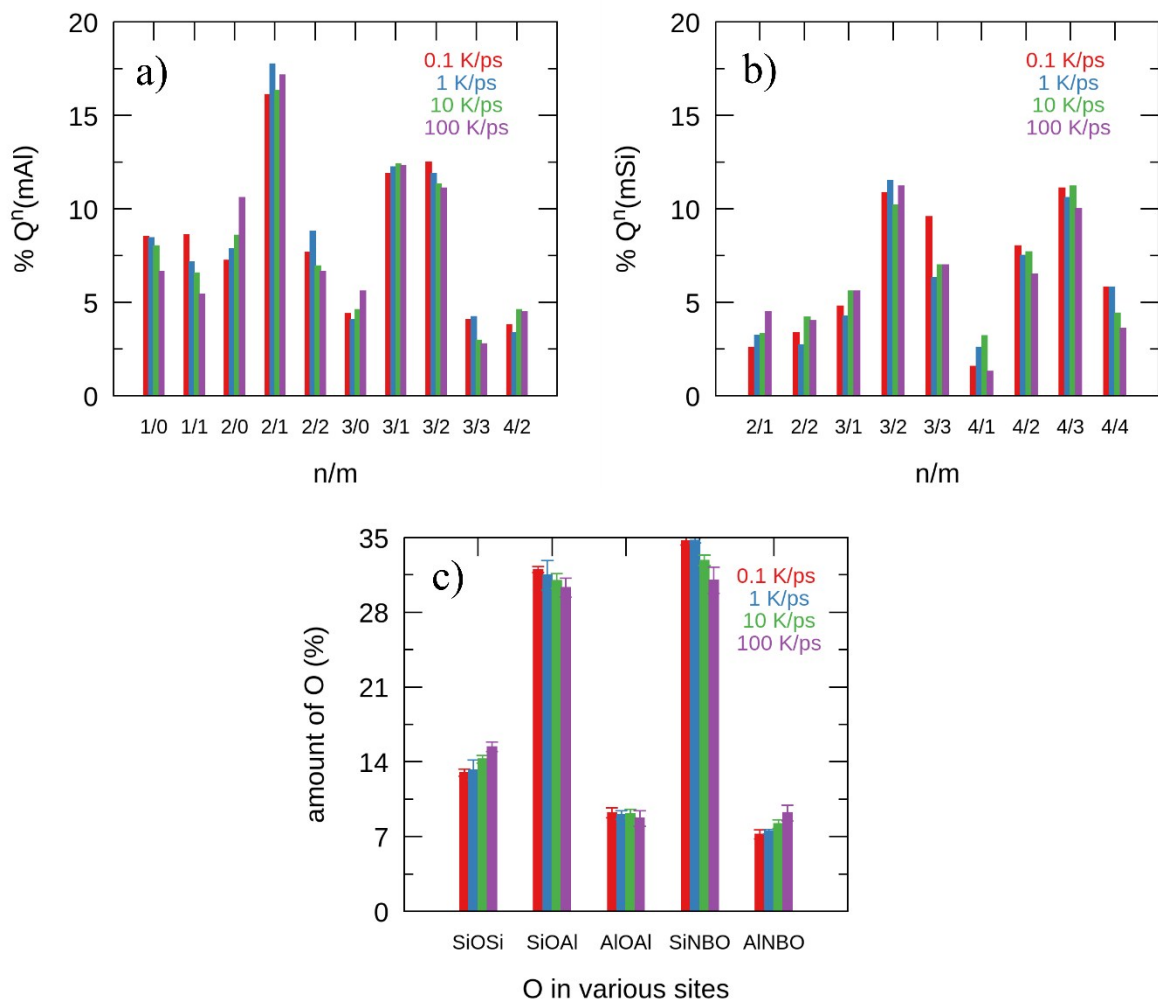


Figure S2: A comparison of (a) Q_{Si} and (b) Q_{Al} unit distribution, and (c) amount of O in various sites for glasses prepared with various cooling rates.

A systematic study of the influence of cooling rate on the distribution of network cations has been studied by considering the cooling rates of four different orders of magnitude. The distribution of Si and Al atoms are shown in Figs. S2 (a) and (b),

respectively. The $Q_{Si}^1(0Al)$, $Q_{Si}^1(1Al)$, $Q_{Si}^2(2Al)$, $Q_{Si}^3(2Al)$ and $Q_{Si}^3(3Al)$ unit population was increased with decreasing cooling rate; however, the increment is very small. Overall, the distribution of units is very consistent within a small error bar. Figure S2 (c) shows the amount of O existing in various sites. The amount of O in Si–O–Si and Al–NBO sites decrease with decreasing cooling rate; however, the changes are very small.

S4: Influence of system size

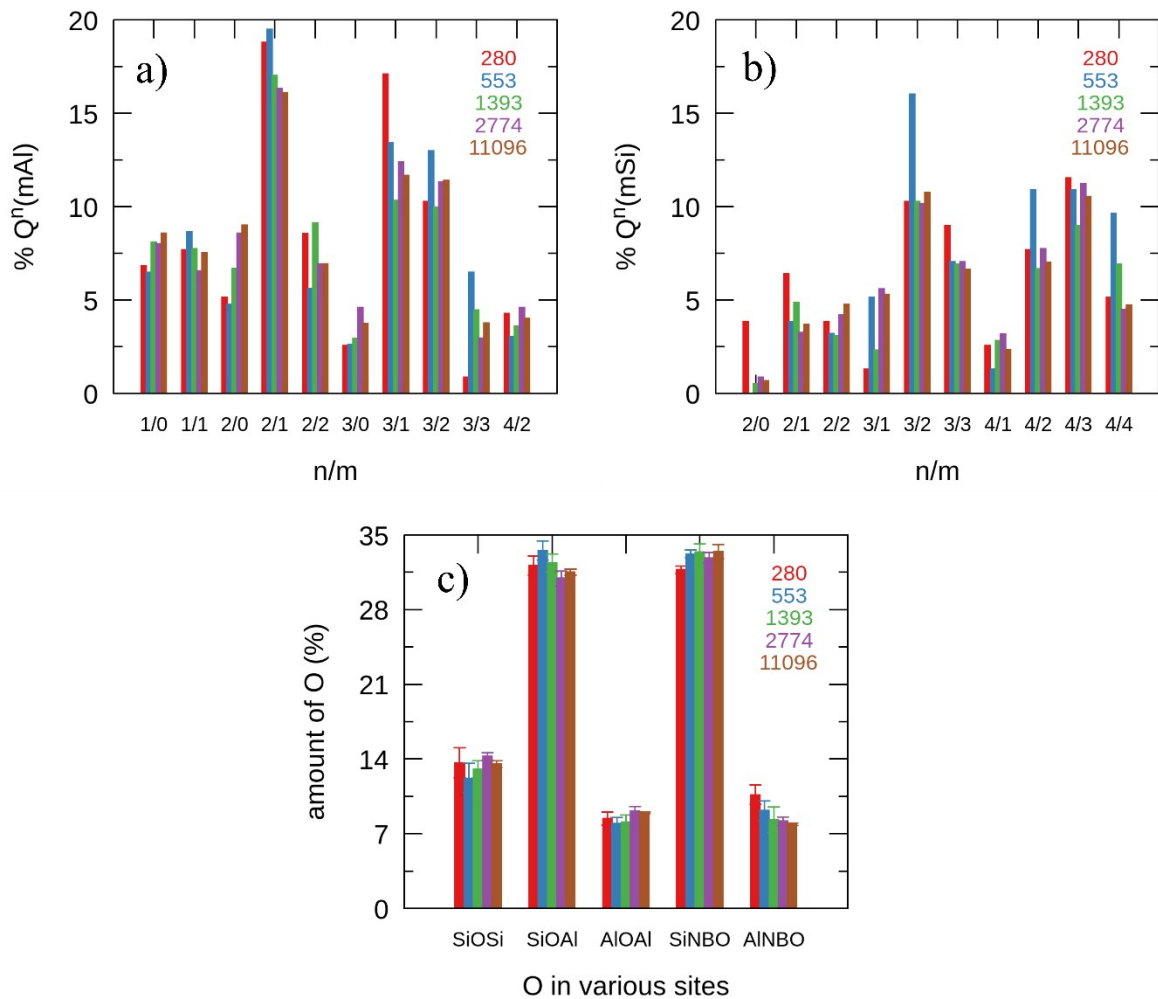


Figure S3: A comparison of (a) Q_{Si} and (b) Q_{Al} unit distribution and (c) amount of O in various sites for glasses of various size (the size is given by the total number of atoms contained in the sample).

Systematic studies of the influence of the sample size on structural properties have been performed. For this purpose, a total of five samples with different number of atoms are prepared with a cooling rate of 10 K/ps using the Pedone potential. The distribution of Si and

Al with respect to network-forming cations are studied and shown in Figure S3 (a) and (b), respectively. It is apparent that the distribution of cations is greatly influenced by the system size and a threshold of the system size has been found. The samples containing more than 1393 atoms show a consistency in the distribution of atoms. As the system size become smaller, the difference in the distribution with the large sample as well as the standard deviation both increase. This is because, in a smaller sample, the numbers of Al atoms are low and thus there are not enough atoms for the statistical distribution for all 15 types of Al units. Figure S3 (c) shows the amount of O present in various sites. The amount of O in Al–NBO decreases with increasing system size, but the decrement is very small. Overall, the system size does not have a significant influence on the O-site population.

S5: Comparison of as-quenched (NVT) and stress-relaxed (NPT) samples

Three glass samples of CMAS are quenched from 5000 to 300 K with a cooling rate of 0.1 K/ps using an NVT ensemble as described in the methods section with three different starting configurations. The samples accumulate a finite amount of stress at 300 K after immediately quenching but these samples have a density equivalent to experimental density as the volume is kept fixed during quenching. These samples are termed as as-quenched samples. In order to remove any other mechanically induced structural changes, these samples are further equilibrated at 300 K with zero stress for about 200 ps using the NPT ensemble. The samples at the end of the 200 ps run are labelled stress-relaxed samples. The averaged structural properties are computed for both the samples and the results are shown in Fig. S4. The stress-relaxed samples exhibit a density 1.4% higher than that of the as-quenched samples with a density of 2.91 g/cm³. Although, a minor change is observed in the density of the two glasses: Figs. S4 (a), (b) and (c) show that there is no significant change in the middle range order of the two glass samples. Similarly, Fig. S4 (d) shows that the pair

distributions of the two glass samples overlap, showing that neither is the stress release affected with short-range order. From these plots it can be concluded that the structural topology is not changed and thus the amount of Al–O–Al or any other unit is almost unaffected by the stress release. The change in density is most probably associated with the bond angles.

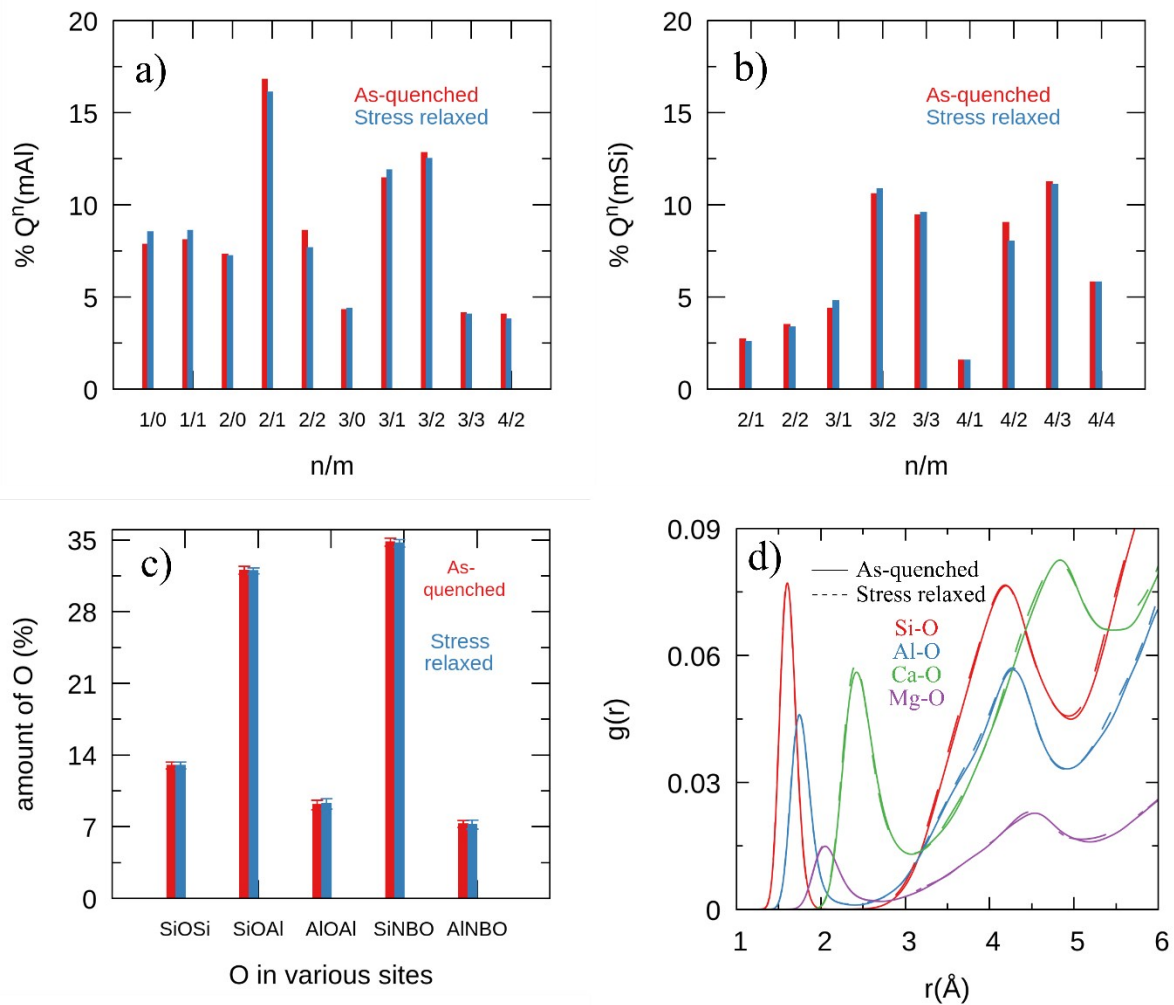


Figure S4: Structural properties of as-quenched and stress-relaxed samples: A comparison of (a) Q^{Si} and (b) Q^{Al} distributions; (c) the amount of O in different sites; (d) partial pair distribution of various cations to O is made for the as-quenched and stress-released samples.

S6: Triclusters

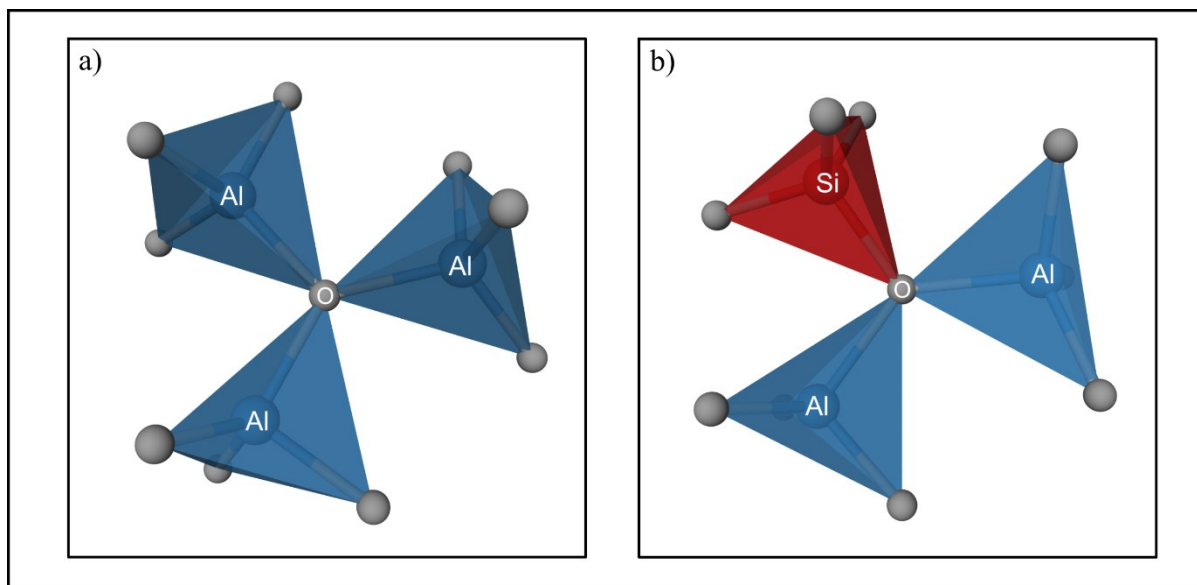


Figure S5: Schematic representation of formation of individual (a) OAl_3 and (b) OAl_2Si triclusters.

S7: ^{27}Al STMAS spectra

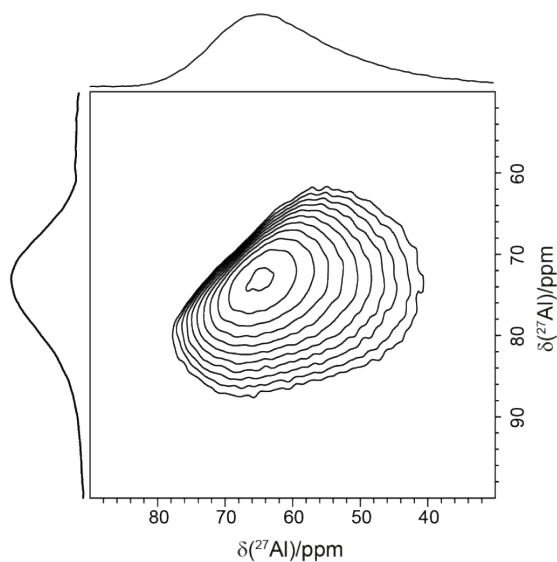


Figure S6: DQF-STMAS-split-t1 spectra of CMAS glass acquired on a Bruker Avance-III HD operating at a B_0 field of 14.1 T with a spinning speed of 20 kHz using a 3.2 mm MAS HFX Y quadruple resonance probe (Bruker)³.

References:

- 1 E. Yildirim and R. Dupree, *Bull. Mater. Sci.*, 2004, **27**, 269–272.
- 2 K. E. Kelsey, J. R. Allwardt and J. F. Stebbins, *J. Non. Cryst. Solids*, 2008, **354**, 4644–4653.
- 3 A. R. Allu, S. Balaji, D. U. Tulyaganov, G. C. Mather, F. Margit, M. J. Pascual, R. Siegel, W. Milius, J. Senker, D. A. Agarkov, V. V Kharton and J. M. F. Ferreira, *ACS Omega*, 2017, **2**, 6233–6243.